Frontiers in Bioscience Landmark

Front. Biosci. (Landmark Ed) **2023**; 28(12): 365
https://doi.org/10.31083/j.fbl2812365

Original Research

Transcriptome and Pathway Analysis Reveals that Adipose-derived Stem Cells Target Inflammatory Factors and Delay the Progression of Diabetic Liver Disease

Yanli Hou[1,2,3,†], Guoliang Gao[1,2,3,4,†], Wenyu Ding[1,2,3], Peishan Wu[1,2,3,4], Changqing Liu[4], Dong Lin[4], Deshan Liu[5,*], Xiaolei Wang[6,1,2,3,*]

[1]Endocrine and Metabolic Diseases Hospital of Shandong First Medical University, 250062 Jinan, Shandong, China
[2]Shandong Institute of Endocrine and Metabolic Diseases, 250062 Jinan, Shandong, China
[3]Jinan Key Laboratory of Translational Medicine on Metabolic Diseases, 250062 Jinan, Shandong, China
[4]Shandong First Medical University, 250018 Jinan, Shandong, China
[5]Department of Traditional Chinese Medicine, Qilu Hospital, Cheeloo College of Medicine, Shandong University, 250012 Jinan, Shandong, China
[6]Shandong University of Traditional Chinese Medicine, 250355 Jinan, Shandong, China
*Correspondence: liudeshan@sdu.edu.cn (Deshan Liu); daturawing@163.com (Xiaolei Wang)
[†]These authors contributed equally.

Academic Editor: Geun-Shik Lee
Submitted: 25 July 2023 Revised: 8 September 2023 Accepted: 12 September 2023 Published: 29 December 2023

Abstract

Background: Diabetic liver disease is one of the main complications that leads to the aggravation of diabetes, but it has not received sufficient attention. This study aimed to provide a better understanding of the altered molecular networks in in diabetic rats with liver damage after stem cell therapy. To a certain extent, our research would be instructive, since almost no studies of this kind have been performed on patients with diabetic liver disease after stem cell therapy. **Methods**: Streptozotocin-induced diabetic rats were treated with adipose-derived stem cells. RNA-Seq analysis was performed on the liver tissues of these animals, and key pathway factors were further identified and validated. **Results**: RNA-Seq analysis revealed numerous affected signaling pathways and functional categories. The results showed that the network of dual specificity phosphatase 1 (*DUSP1*), an oxidative stress-related gene, was prominently activated in the liver after stem cell therapy, and the enrichment of genes associated with liver damage, steatosis and fibrosis was also detected. The extracellular regulated protein kinase (ERK)/signal transducer and activator of transcription 3 (STAT3) signaling pathway may be involved in this process by regulating the nucleotide-binding and oligomerization domain-like receptor family pyrin domain-containing 3 (NLRP3) inflammasome. **Conclusions**: These data provide novel insights into liver biology, suggest common alterations in the molecular networks during diabetic liver damage, and show the advantages of stem cell therapy, indicating its further application potential for early treatment of diabetic liver damage and delaying the progression of liver fibrosis in the later stage.

Keywords: diabetic liver disease; adipose-derived stem cells; *DUSP1*; ERK; NLRP

1. Introduction

Diabetes mellitus (DM) is one of the most common chronic diseases in the world, and its global prevalence has more than doubled in the past 20 years [1,2]. The traditional complications of diabetes are well known for their prolonged effects and heavy burdens. Complications were once limited to vascular disease, but advances in diagnosis and treatment have brought complications such as cognitive decline, obstructive sleep apnea, and liver disease into view [3]. Recent studies have shown that among individuals with diabetes worldwide, more than half have nonalcoholic fatty liver disease (NAFLD), and nearly half have nonalcoholic steatohepatitis (NASH) [4]. Liver damage or fibrosis, which are major complications of diabetes, can cause serious and irreversible consequences over time, including liver cirrhosis and liver cancer [5], which may also endanger patient lives. Decades of extensive research and clinical trials have resulted in a detailed protocol for the treatment of these diseases, but the specific mechanism remains unclear, greatly limiting early intervention and the prevention and treatment of complications.

Stem cell injection has been widely used to treat hematological diseases, autoimmune diseases and other diseases. Furthermore, based on the current epidemic trend in COVID-19, stem cells have shown great potential in the prevention and treatment of COVID-19 and related sequelae [6–8]. In patients with type 1 diabetes mellitus (T1D)-induced depletion of islet beta cells (β-cells), insulin secretion is completely inadequate, and stem cell transplantation can repair damaged areas. Stem cells can be induced to differentiate into insulin-producing cells (IPCs) and improve the function and proliferation of resident pancreatic islets [9]. Stem cell therapy also has good therapeutic effects on various complications of diabetes, such as protecting against T1D-mediated renal injury and alleviating podocyte

injury in diabetic kidneys [10]. In a previous study, we demonstrated the therapeutic effect of adipose-derived stem cell (ADSC) injection on diabetes by examining the complications of changes in the liver [11]. We found that stem cells could exert their therapeutic effects by improving mitochondrial permeability transition pore (MPTP) opening, but the specific mechanisms need further examination. In this study, we aimed to further explore the role of mitochondrial function changes in diabetic liver diseases, explore the specific mechanisms and key targets, and provide new ideas for the clinical application of related drugs.

In recent years, transcriptomic analyses of diabetes models have revealed multiple possible targets for, which is consistent with our transcriptome sequencing results. Se novo germline gain-of-function (GOF) mutations can occur accidentally in the transcriptional regulator signal transducer and activator of transcription 3 (STAT3), which is one of the rarer causes of diabetes. A specific class of $CD8^+$ T cells is inhibited when STAT3 activity is normal, and once this process becomes abnormal, it can lead to the occurrence of diabetes [12]. On the other hand, neurogenic hormone 3 (ngn3) has been shown to be associated with adult β-cell transition, which suggests that this factor may be a potential target for treating DM [13]. Interestingly, recent studies of the transcriptional landscape in human adipocytes from healthy individuals of different sizes and type 2 diabetes mellitus (T2D) patients suggest that excessive mitophagy caused by activation of the mitochondrial reactive oxygen species (ROS) pathway and nuclear factor kappa B (NF-κB) signaling may be associated with T2D with hepatic insulin resistance and hepatic steatosis [14]. In addition, several studies have indicated a possible association between differences in serum fibroblast growth factor 1 (Fgf1) levels and the onset of diabetic cardiomyopathy, which may be a novel use of this target in the field of metabolic disorders [15]. The nucleotide-binding and oligomerization domain-like receptor family pyrin domain-containing 3 (NLRP3) inflammasome is the key sensor of cytolytic pathogens or stress signals, and its activity is tightly controlled [16]. After being stimulated, the inflammasome induces the production of active caspase-1 and the subsequent activation of proinflammatory cytokines, including interleukin (IL)-18 and IL-1β. The NLRP3 inflammasome has been implicated in multiple diseases, including diabetes and liver diseases [17]. Our previous study showed that the NLRP3 inflammasome was affected by ADSC treatment [11], but the signaling pathways involved are unclear.

Advances in transcriptome analysis are furthering our understanding of diabetes. In the current study, we compared the RNA-seq results of treated and untreated streptozotocin-induced diabetic rats, analyzed the expression status of each factor and identified multiple potentially significant networks. Our data showed the transcriptomic changes and networks in diabetic rats after ADSC treatment, and we further validated the results using the human hepatoma cell line HepG2 *in vitro*, setting the foundation for further identification of therapeutic targets for diabetic liver damage.

2. Materials and Methods

2.1 Isolation and Characterization of ADSCs

ADSCs were isolated as described previously [11]. In brief, white adipose tissue from the inguinal region of rats was placed in a digestion solution containing 0.1% collagenase type I and subjected to continuous agitation at 37 °C for 1 h. The reaction was stopped by the addition of culture medium, and the cell suspension was centrifuged at 2000 rpm for 10 min. The acquired cells were resuspended and filtered through 100-µm filters. After being washed twice, the cellular precipitate was resuspended in cell culture medium and cultured in 25 mm^2 cell flasks at 37 °C in a 5% CO_2 incubator. The cells were cultured in DMEM containing 1 g/L glucose (#11885084, Gibco, Carlsbad, CA, USA), 10% fetal bovine serum (#10099141C, Gibco, Carlsbad, CA, USA) and 1% penicillin/streptomycin at 37 °C in 5% CO_2, and the medium was changed twice per week. The cells were observed daily under an inverted phase contrast microscope. The cells were detached with 0.25% trypsin/0.01% EDTA and replated for passaging. We observed that third-generation ADSCs adipogenic and osteogenic differentiation potential, and the immunophenotype of surface markers was examined by flow cytometry. ADSCs of this generation and the following two generations were used in the experiments.

2.2 Animal Experiment

All studies were performed in accordance with the National Institute of Health guidelines and were granted formal approval by the Research Ethics Committee of Shandong Institute of Endocrine & Metabolic Diseases. Male 8-week-old SD rats were exposed to 12 h of light/darkness under constant temperature and humidity and had free access to water and regular food. All of the rats had similar body weights and growth statuses before streptozotocin (STZ) administration. Twenty rats were fasted for 16 h (with free access to water) and were then intraperitoneally injected with 60 mg/kg STZ (#S8050, Solarbio, Beijing, China). After the injection, the rats were allowed to roam free for three days to stabilize the results. Fasting blood glucose levels were taken from the tail tip and measured daily using a glucometer until both blood glucose measurements were above 16.7 mmol/L. At this time, the rats were diagnosed with STZ-induced diabetes, which was set as day 0 of the experiment. Fourteen days later, the rats were randomized again. One group was the ADSC treatment group (ADSC group), and these rats received 2.0×10^6 ADSCs through the tail vein, while the other group was the diabetes group (DM group) and received the same dose of PBS. Body weight and blood glucose levels in the two groups were dynamically monitored weekly. After 6 weeks of ADSC treatment

Table 1. Oligonucleotide primers used for quantitative reverse transcription–polymerase chain reaction (qRT–PCR).

Gene symbol	Accession	Forward primer (5′-3′)	Reverse primer (5′-3′)
myelin basic protein (*Mbp*)	NM_001025289	CAGCACCGCTCTTGAACACC	TGCCTCCCCAAACACATCACT
lymphocyte antigen 6 complex, locus A-like (*Ly6al*)	NM_001128099	CCATATTTGCCTTCCCGTCT	CAGGATGAACAGAAGCACCC
acid phosphatase 3 (*Acpp*)	NM_001134901	CCAGAACGAGCCCTACCCA	AGAACAAGCAGCAATATCACC
2′-5′ oligoadenylate synthetase 1F (*Oas1f*)	NM_001009490	TCACCTCCCTGCTGACACC	TGTTCGCCCATCACAACCC
amylase 2a3 (*Amy2a3*)	NM_031502	ATGACCCACACACTGCGGATG	TGCACCCCTCCAAATCCCT
one cut homeobox 1 (*Onecut1*)	NM_022671	AATTCAGGCAACTCTTCGTCT	CGTGGTTCTTCCTTCATGCTT

or control treatment, the rats were anesthetized after being fasted; blood was collected from the jugular vein, and tissue samples were collected prior to sacrifice.

2.3 RNA-seq Analysis

A TRIzol kit (#15596026, Thermo Fisher Scientific, Waltham, MA, USA) was used to extract total RNA from liver tissue according to the manufacturer's instructions. The total RNA concentration was determined by a NanoDrop microvolume spectrophotometer (Thermo Fisher Scientific, Waltham, MA, USA). The ratio of OD260 to OD280 was considered an indicator of RNA purity. In addition, we used agarose gel electrophoresis to ensure RNA integrity and exclude gDNA contamination.

RNA-seq analysis was performed by Health Biotechnology (Shanghai, China). Briefly, the NEBNextTM Ultra II Directional RNA Library Prep Kit was used to construct sequencing libraries for validation and quantification. The Illumina HiSeq X platform was then used for 150 bp peer sequencing. The expression level of each gene was estimated by calculating sequences mapped to reference sequences (reads), of which the most commonly used method is read per million transcripts per kilobyte (RPKM). In the DEGseq v1.20.0 software package, the differentially expressed genes (DEGs) were analyzed using the random sampling (MARS) model. Differences in gene expression among samples were considered significant when all of the following conditions were met: fold change (FC) >2 or <0.5, false discovery rate (FDR) q value <0.05 and RPKM >2 for at least one sample.

2.4 Cell Culture and Treatments

The human hepatoma cell line HepG2 was provided without Mycoplasma contamination and authenticated using short tandem repeat (STR) profiling analysis by Procell Life Science & Technology (Wuhan, China) under the catalog number CL-0103. The cells were maintained in DMEM supplemented with 10% fetal bovine serum and 50 U/mL penicillin/streptomycin in an incubator under a humidified atmosphere of 5% CO_2 and 95% air at 37 °C. We used H_2O_2 treatment to simulate oxidative stress *in vitro* and observed the effects of ADSC culture supernatant and hepatocyte growth factor (HGF), which is a cytokine secreted by ADSCs, on inflammation and oxidative stress.

HepG2 cells were plated in 6-well plates at 1×10^6 cells/well and grown in medium for 24 h. Then, the cells were pretreated with or without ADSC supernatant, HGF (10 ng/mL), or the extracellular regulated protein kinase (ERK)1/2 inhibitor U0126 (2 µM) for 2 h and were cultured with H_2O_2 (600 µM) for another 6 h to determine the effect of ADSCs on ROS-induced inflammation.

2.5 Western Blotting

To obtain whole protein extracts, rat livers were treated with lysis buffer containing protease and phosphorylation inhibitors. The stained membranes were scanned using the Odyssey CLx imaging system (LI-COR, Lincoln, NE, USA) to measure the fluorescence at 800 nm and 700 nm. The fluorescence intensity of the bands was also quantified with the Odyssey CLx imaging system, and the results are expressed as the fold change relative to the control after normalization to the respective internal control. Antibodies against P-ERK1/2 (#4370), ERK1/2 (#4695), P-P38 (#4511), P38 (#8690), P-c-jun N-terminal kinase (JNK) (#9255), JNK (#9252), P-STAT3 (#9145), STAT3 (#9139), GAPDH (#5174) and β-tubulin (#86298) were obtained from Cell Signaling Technology (CST, Danvers, MA, USA) and used for western blotting.

2.6 Quantitative Reverse Transcription–Polymerase Chain Reaction (qRT–PCR)

Using the QuantiTect Reverse Transcription Kit (QIAGEN, Hilden, Germany), total RNA in each sample was reverse transcribed into cDNA. Using the Light Cycler system, the resultant cDNA was used as a template for real-time quantitative PCR. Nonspecific amplification was used to perform melt curve analysis. The data were normalized to β-actin, which was used as an internal control for normalization. The oligonucleotide primers used in this study are shown in Table 1.

2.7 Gene Enrichment Analysis, Upstream and Downstream Analyses and Interaction Network Modeling

The gene expression data were input into Ingenuity Pathways Analysis (IPA) software (Ingenuity Systems; https://ingenuity.com/) to establish a causal network. Upstream regulator analysis, downstream effect analysis and mechanistic network analysis were performed to determine likely causal mechanisms, and the p value was network-bias-corrected.

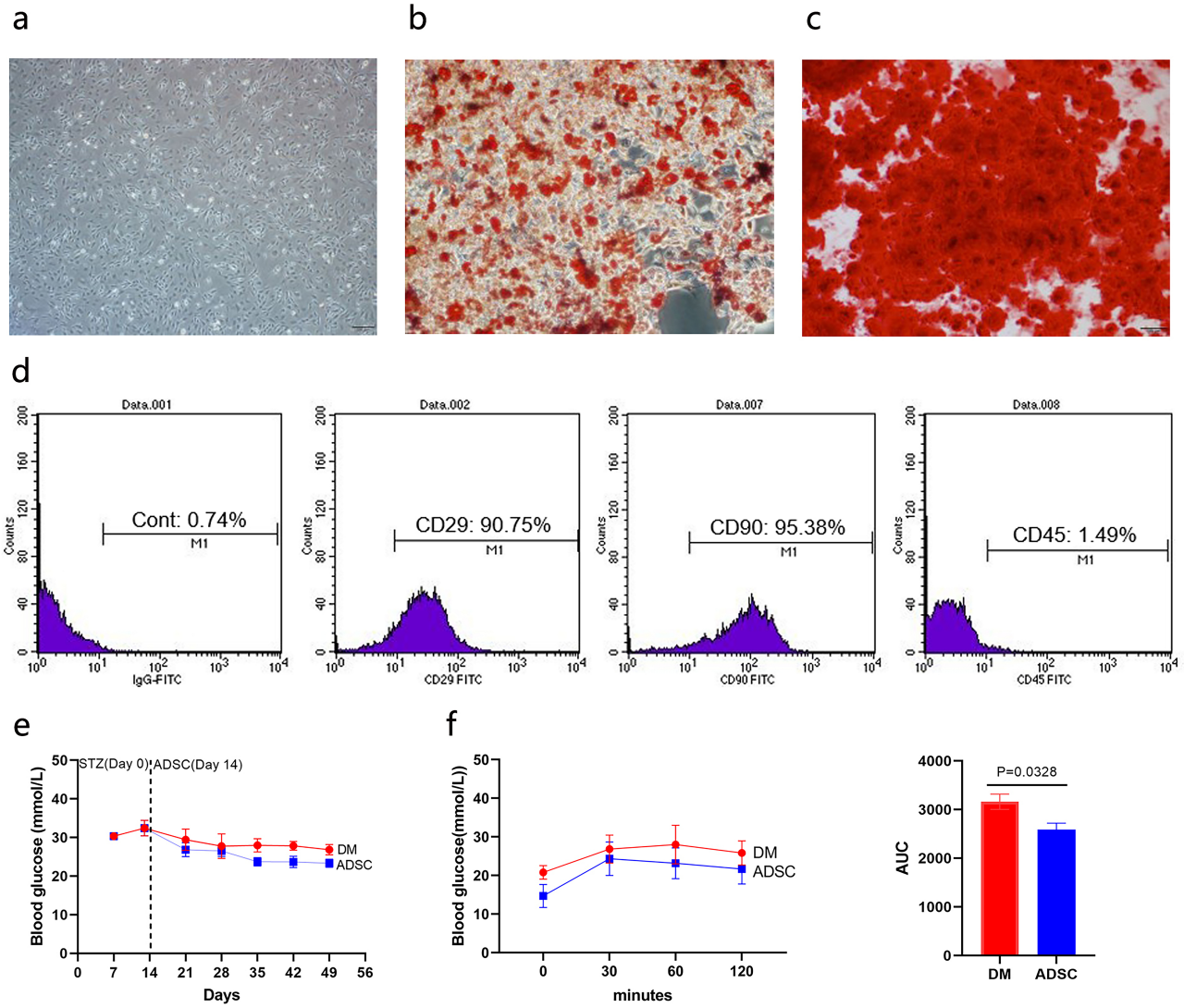

Fig. 1. Characteristics of ADSCs and physiological differences between the two groups. (a) Morphology of ADSCs at Passage 3 (×40). (b,c) Differentiation potential of ADSCs into adipocytes and osteoblasts, as shown by Oil Red O and Alizarin Red staining (×100). (d) Surface markers of ADSCs, as shown by flow cytometry. (e) Blood glucose levels in rats were measured weekly. The day on which STZ-induced diabetes was established in rats was referred to as day 0 of the experiment. ADSCs were injected at the end of the second week. (f) OGTT results before the rats were sacrificed and the AUC. DM, Diabetes mellitus; ADSCs, adipose-derived stem cells; STZ, streptozotocin; OGTT, Oral glucose tolerance test; AUC, area under the curve.

2.8 Statistical Analysis

The analyses were performed using Microsoft Excel 2021 and GraphPad Prism 9.0 software (San Diego, CA, USA). The results are reported as the mean ± SD. Comparisons of between groups were performed using unpaired *t* tests. $p < 0.05$ was considered significant for the qRT–PCR and western blot data.

3. Results

3.1 RNA-Seq-Derived Gene Expression Profiles and Related Pathways

Fig. 1a–d shows that ADSCs had adipogenic and osteogenic differentiation potential and were positive for CD29 and CD90 (90.75% and 95.38%) and negative for the leukocyte antigen CD45 (1.49%). These cells met the criteria for ADSCs. The weekly blood glucose levels and the oral glucose tolerance test (OGTT) results before the rats were sacrificed are shown in Fig. 1e,f. There was no significant change in the blood glucose levels between the two groups; however, the area under the curve (AUC) of the OGTT was reduced in the ADSC group compared to the DM group. Moreover, ADSC treatment alleviated hepatic injury in our previous study [11].

To examine the effect of stem cell therapy on the transcriptional landscape, we performed full transcriptome RNA-seq analysis on the liver tissues of those STZ-induced

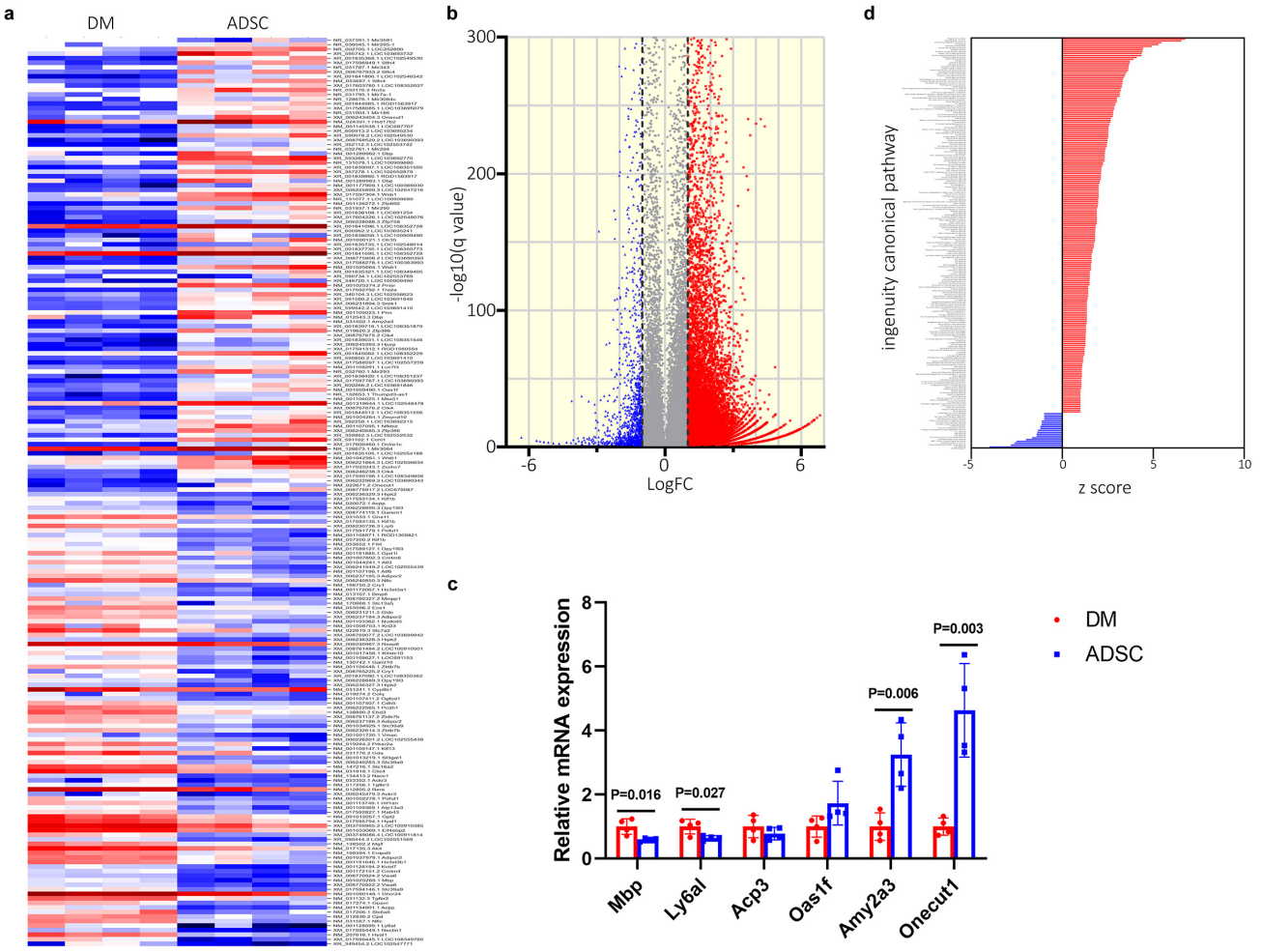

Fig. 2. DEGs in the two groups. (a) Heatmap showing DEG levels (2.0 FC, FDR $p < 0.05$) in the liver tissues of eight rats based on the RNA-seq data. Different columns indicate different samples, and different rows indicate different transcripts. The color scale represents the expression level of each gene in a single sample. If not otherwise noted, the terms upregulated or downregulated are used to describe the changes in stem cell-treated animals compared to untreated animals. (b) Volcano plot showing the RNA-seq data from the two groups, with $p < 0.05$ and $|\log FC| > 0.5$ as the cutoff criteria. The blue dots indicate downregulated genes, the red dots indicate upregulated genes, and the gray dots indicate genes without significant differences in expression. (c) The expression levels of selected genes in the liver tissues of eight untreated and stem cell-treated diabetic rats were measured by qRT–PCR. The data are presented as the mean ± S.E. values. (d) Significantly affected ($2.0 < Z$ score < -2.0) canonical pathways were automatically generated by IPA. The horizontal bars show the different pathways calculated based on the Z score. Red represents activation, while blue represents suppression. DM, STZ-induced DM rats; ADSC, ADSC-treated DM rats; DEGs, Differentially expressed genes; FC, fold change; FDR, false discovery rate; IPA, Ingenuity Pathways Analysis.

hyperglycemic rats. Fig. 2a shows liver transcriptome differences in diabetic rats with or without treatment. With $p < 0.05$ and $|\log FC| > 0.5$ as the cutoff criteria, a total of 1770 upregulated transcripts and 362 downregulated transcripts were screened (Fig. 2b). We selected certain highly altered upregulated (*Mbp*, *Ly6al*, *Acpp*) and downregulated (*OAas1f*, *Amy2a3*, *Onecut1*) genes from the RNA-seq data and verified them by qRT–PCR (Fig. 2c). The results were consistent with the RNA sequencing results.

Examining the upregulated gene transcripts into IPA and performing canonical pathway analysis showed that many pathways were activated or inhibited during this process, including the hepatic fibrosis signaling pathway, IL-6 signaling pathway, and insulin receptor signaling pathway, which were significantly enriched (Fig. 2d) and showed the ameliorative effect of stem cell treatment on liver damage, inflammation, and insulin secretion.

3.2 The Effects of ADSCs on Hepatotoxicity-Related Functions

IPA of downstream effectors can be used to predict comprehensive increases or decreases in downstream biological activity and gene-related function based on the causal relationship between measured transcriptome level

changes and these activities and functions. **Supplementary Fig. 1a** shows a high level of middle and downstream activity and function in the liver tissue of treated and untreated diabetic rats. Fig. 3 shows multiple functional categories that were enriched, such as liver pathological changes and metabolic disorders, which included liver tissue alterations, cell growth and proliferation disorders, and suggested that stem cells could improve liver function and liver injury in DM. Furthermore, functional categories associated with immune system diseases and endocrine system diseases showed significant alterations. Notably, functional categories associated with hepatotoxicity showed significant upregulation, and there were much greater increases than those associated with nephrotoxicity and cardiotoxicity (Fig. 3b and **Supplementary Fig. 1b**). Liver toxicity was mainly characterized by liver damage, hepatitis, liver steatosis, liver fibrosis (LF) and other factors (Fig. 3c). Taken together, our data revealed significant decreases in susceptibility to liver damage and DM after stem cell therapy.

3.3 A Chemokine Network Indicating Reduced Liver Damage in Diabetes

Multiple liver-related functional categories were enriched in stem cell-treated diabetic rats compared to untreated diabetic rats. Among the differentially enriched categories, liver damage and liver steatosis were the most prominent (Fig. 3c). Fig. 4a shows a heatmap of the $\log_2$ expression values of liver damage-related genes (*Ccl4*, *Abcb1a*, *Cblb*, *Cnr2*, *Ddit3*, *Hmgb*, *Igf1*, *Il18*, *Irf3*, *Mapk14*, *Nr1i3*, *Sdc4*, *Sirt1*, *Gsk3b*, *Tgfbr2*, *Stk24*, *Klf2*, *Mboat7* and *Cps1*) in rat liver tissue. Our previous study showed a strong correlation between *TGFB* expression and the progression of liver damage [11], which was consistent with the results of this analysis. Overall, the expression of *Ccl4*, *Abcb1a*, *Cblb*, *Cnr2*, *Ddit3*, *Hmgb*, *Igf1*, *Il18*, *Irf3*, *Mapk14*, *Nr1i3*, *Sdc4* and *Sirt1* in hepatocytes promoted the progression of liver damage in mice, and *Gsk3b*, *Tgfbr2*, *Stk24*, *Klf2*, *Mboat7* and *Cps1* expression alleviated liver damage in mice. Interestingly, *MAPK14* has previously been shown to alleviate liver damage [18]. This may explain the bidirectional alterations in MAPK14 isoform expression in our data.

Moreover, some genes associated with liver steatosis were downregulated in stem cell-treated diabetic rats compared to untreated diabetic rats (*Acbd5*, *Bhlhe40*, *Casp2*, *Cnr2*, *Ddit3*, *Dnajc7*, *Egfr*, *Helz*, *Ifit2*, *Il18*, *Irf3*, *Isg15*, *Isg15*, *Lime1*, *Nr1i3*, *Ptpn2*, *Sirt1*, *Srsf2*, *Tp53inp1*, *Thra*, *Egfr*, *Epas1*, *Foxo1*, *Gldc*, *Gna11*, *Gpam*, *Insig2*, *Insr*, *Klf2*, *Lrp6*, *Mapk14*, *Mboat7*, *Mgll*, *Acox1*, *Adipor2*, *Atf6*, *Stk24*, *Pdpk1* and *Plin2*; Fig. 4b). Interestingly, our data suggest that the progression of liver damage and hepatic lipid accumulation may be ameliorated by the inhibition of *Cnr2*, *Ddit3*, *Il18*, *Irf3*, *Mapk14*, *Nr1i3* and *Sirt1* following stem cell therapy.

3.4 Upstream Regulator Analysis and Mechanistic Network Analysis Predict that Dual Specificity Phosphatase 1 (DUSP1) Plays anImportant Role in the Effects of Stem Cell Treatment on DM

Upstream regulator analysis can predict upstream molecules. Thus, we identified relevant factors by which stem cell therapy inhibits processes related to liver damage. IPA was used to predict possible factors, resulting in 30 factors with a |Z score| greater than 3 (Table 2). These 30 factors were examined by IPA, and the nine factors shown in Fig. 5a were indirectly associated with liver damage. Among them, *DUSP1* plays an important role in the cytosol and mitochondria. Changes in these factors identified by RNA-seq (Fig. 5b,c) were analyzed and showed that IPA predicted the importance of DUSP1 in the effects of stem cell treatment on diabetes.

Table 2. Upstream regulators predicted by IPA.

Upstream Regulator	|Z score|	*p* value of overlap
P38 MAPK	4.355	3.91×10^{-2}
ZBTB10	4.249	2.73×10^{-3}
Eldr	4.536	4.90×10^{-9}
STRA8	3.207	7.42×10^{-4}
CCNDI	3.200	1.02×10^{-6}
FEV	4.060	3.09×10^{-4}
SOX2	4.076	7.02×10^{-5}
REL	3.181	3.02×10^{-2}
LEF1	3.915	2.06×10^{-4}
STAT4	4.618	4.69×10^{-3}
ISL1	3.207	2.68×10^{-3}
COPS5	3.024	1.00×10^{-2}
INHBA	3.893	2.50×10^{-3}
CREB1	3.095	9.25×10^{-6}
PTGER2	3.916	1.15×10^{-5}
APP	3.091	8.21×10^{-2}
TICAM1	4.907	3.34×10^{-2}
MITF	3.703	1.67×10^{-2}
AHR	3.543	1.76×10^{-4}
MAPK14	3.731	4.06×10^{-2}
KMT2D	3.805	7.16×10^{-4}
NFKB1	3.293	3.07×10^{-2}
ERBB2	3.802	4.57×10^{-1}
MEIS1	3.148	4.13×10^{-2}
TLR3	4.846	4.77×10^{-2}
CBX5	3.289	2.78×10^{-2}
DUSP1	3.435	2.42×10^{-3}
GRIN3A	3.335	3.05×10^{-4}
CITED2	4.259	4.01×10^{-2}

Upstream regulator analysis of DEGs explained the mechanistic networks underlying the observed changes in gene expression during stem cell therapy for DM (**Supplementary Fig. 1**), including the *STAT4* (|Z score| = 4.618), *PTGER2* (|Z score| = 3.916), *LEF1* (|Z score| =

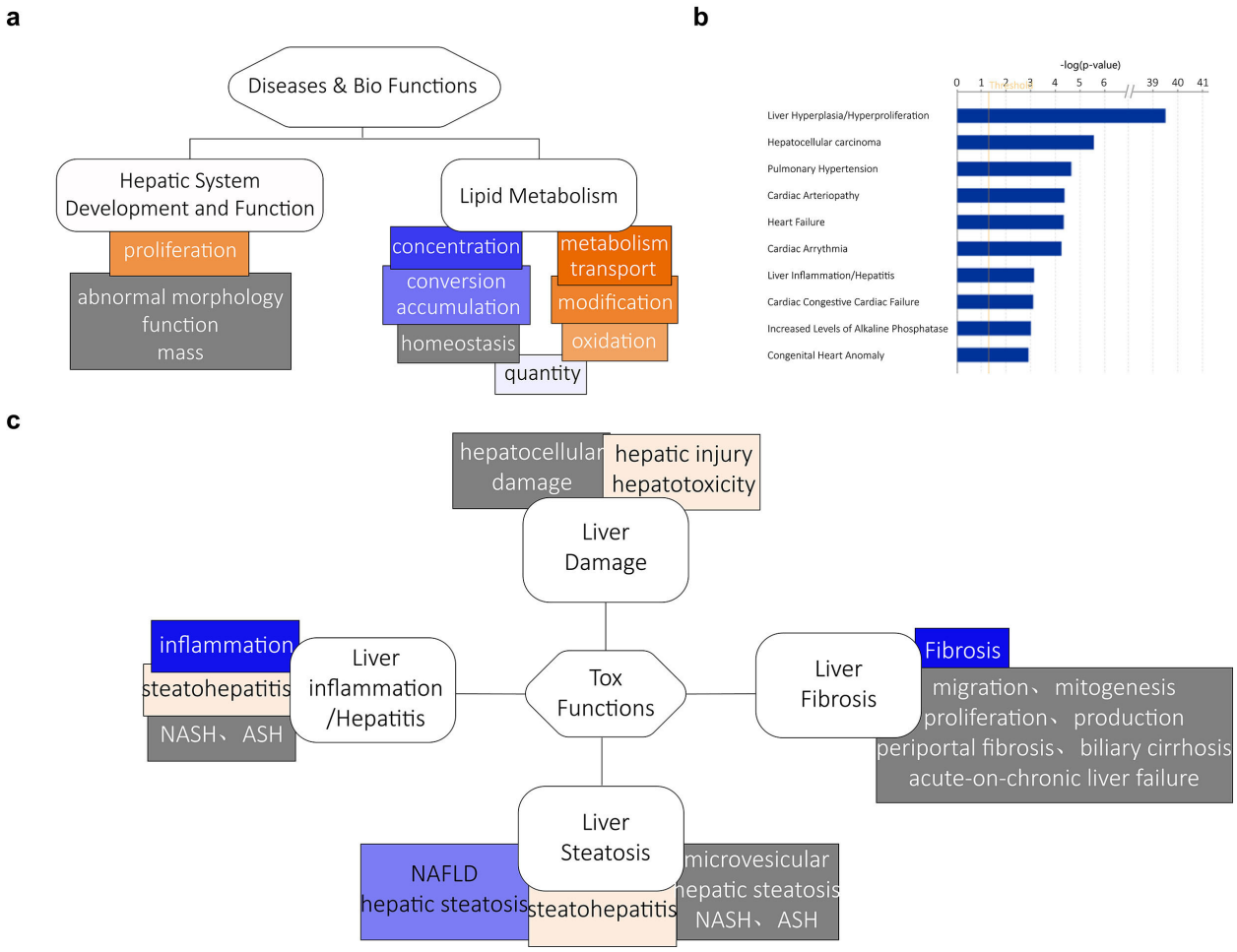

Fig. 3. Downstream effector analysis of the two groups. (a) The affected diseases and biological function categories based on the tree map in **Supplementary Fig. 1a**. (b) The top ten most significantly enriched pathways. (c) The affected hepatotoxicity-related functional categories based on the tree map in **Supplementary Fig. 1b**. The major colored rectangles indicate a family of associated biological functions or diseases; blue indicates a decrease and orange indicates an increase. The sizes (using Fisher's exact test *p* value) of the rectangles indicate whether the category is predicted by IPA to increase or decrease significantly between groups; and higher absolute Z scores are represented by color intensities. NAFLD, nonalcoholic fatty liver disease; NASH, nonalcoholic steatohepatitis; ASH, alcoholic steatohepatitis.

3.915), *INHBA* (|Z score| = 3.893), *AHR* (|Z score| = 3.543), *DUSP1* (|Z score| = 3.435), *CCND1 V* (|Z score| = 3.200), and *CREB1* (|Z score| = 3.095) networks (Fig. 5c, **Supplementary Fig. 2**). *DUSP1* was predicted with relatively high confidence to directly activate the IL-12 complex, IL-1B and tumor necrosis factor (TNF). Furthermore, the activated IL-12 complex was predicted to directly promote the expression of STAT3 and STAT4; moreover, the upregulation of TNF was predicted to activate the vitamin D receptor (VDR) and coactivate SP1 through the upregulation of IL-1B. At the terminus of the mechanistic network, *CREBBP*, *SMAD3*, and *EP300* were activated, and *CDKN2A* was inactivated. In summary, *DUSP1* was highly enriched among the genes in liver damage-related functional categories with relatively high confidence and numerous predicted relationships.

3.5 DUSP1 may Affect Liver Function during Stem Cell Treatment of DM

By analyzing the factors that were downstream of *DUSP1*, the functional networks identified by IPA helped us to identify a mechanistic network in which *DUSP1* affects multiple functions through multiple factors. The network is shown as genes and biological relationships between the nodes and lines, and nodes with specific shapes indicate the regulatory effect determined by IPA. The first network we identified consisted of the DEGs, their upstream and downstream relationships, and the functional changes that might result (32; as indicated in the legend); in short, this network probably moderates sensory system development (Fig. 6a). The other interesting enriched network moderated the antiviral response (Fig. 6b). Interestingly, we identified DUSP1 as a key hub gene in liver damage and

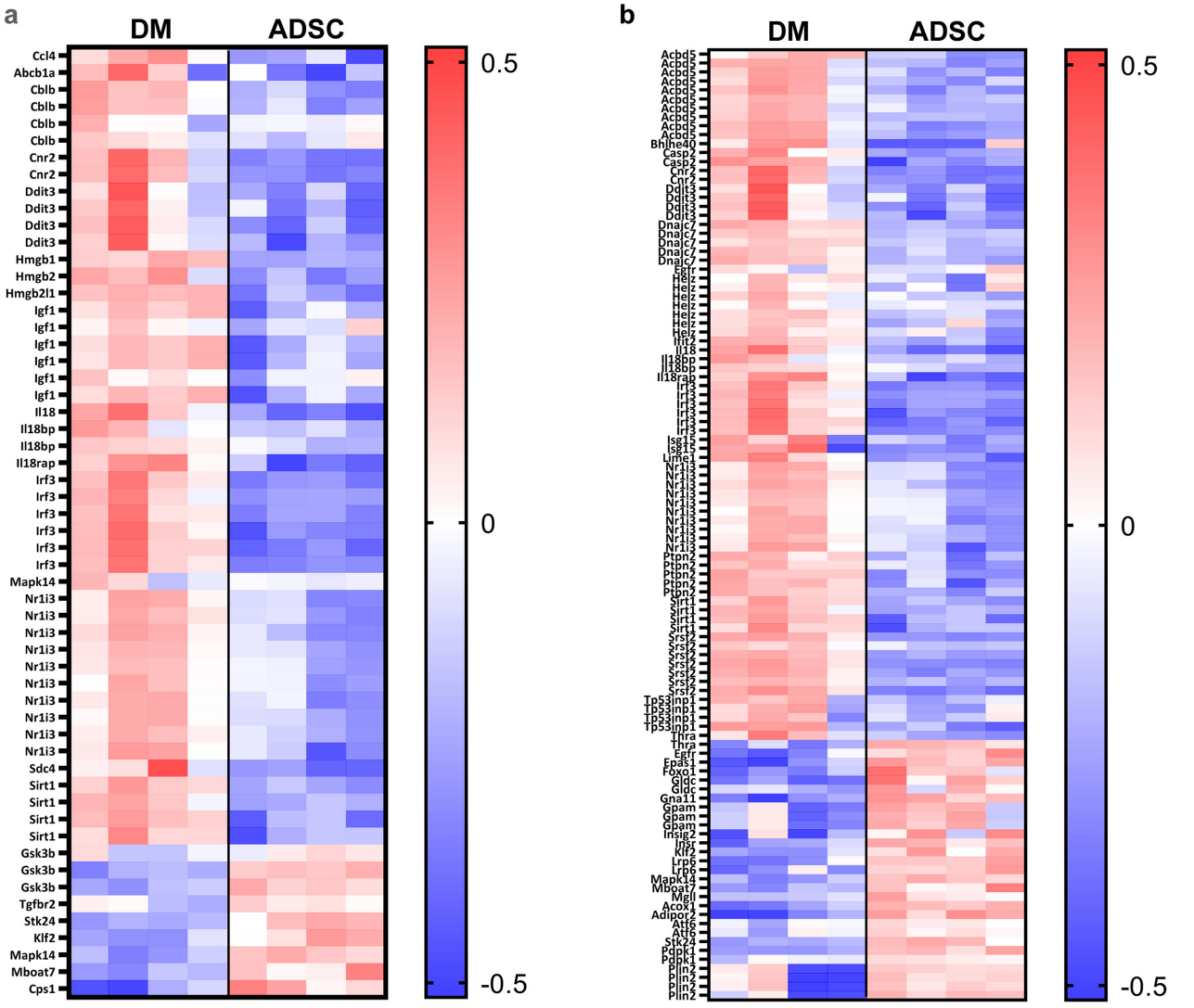

Fig. 4. Heatmap showing the amelioration of liver damage and liver steatosis in diabetic rats. Heatmap showing the expression of several upregulated and downregulated genes related to liver damage (a) and liver steatosis (b) in eight diabetic rats treated with or without ADSCs. The data are presented as the $\log_2$ TPM (transcript per million) expression values. The expression values are shown according to the color scale.

other liver disease networks (Fig. 6c). Furthermore, with the Grow and Path Explorer IPA functions, we confirmed the indirect relationship between *DUSP1* expression and numerous liver diseases (Fig. 6d).

However, we also sought to explore the mechanism by which *DUSP1* causes liver damage. The protein encoded by *DUSP1* can dephosphorylate mitogen-activated protein kinase (MAPK), thus playing an important role in multiple pathological processes. We examined the phosphorylation status of the ERK1/2, P38 and JNK pathways, which are three pathways that play key roles in glucose metabolism disorders, in stem cell-treated diabetic rats compared to untreated diabetic rats. The results showed that the phosphorylation of ERK1/2 was significantly downregulated in ADSC-treated DM rats (Fig. 7a,c). This finding was further confirmed *in vitro*. P-ERK1/2 was increased when HepG2 cells were cultured with H_2O_2. However, it was restored to some extent when the cells were pretreated with HGF or ADSC supernatant, and there was a similar change in response to the ERK inhibitor U0126 (Fig. 7b,d). Moreover, the change in P-STAT3 was similar to that in P-ERK1/2. P-STAT3 was also reduced when the cells were pretreated with an ERK inhibitor. This result suggested that STAT3 phosphorylation was mediated by the ERK signaling pathway. These results suggested that stem cell therapy could act through *DUSP1*-mediated regulation of the ERK/STAT3 pathway.

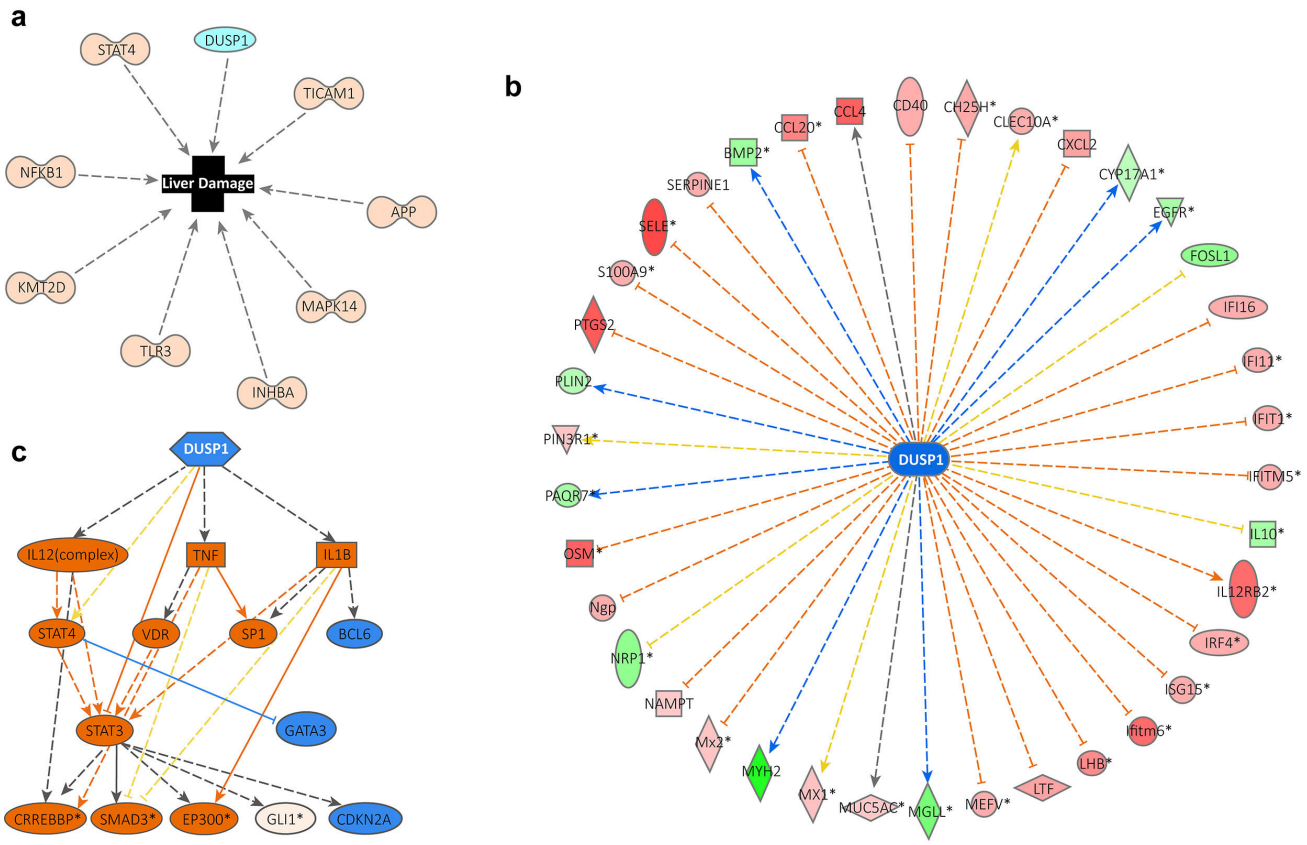

Fig. 5. Upstream regulator analysis and mechanistic network analysis predict multiple affected signaling networks. (a) Upstream regulators that are indirectly associated with liver damage. (b) The possible upstream location of DUSP1 was jointly predicted based on changes in factors associated with DUSP1. (c) DUSP1 mechanism network diagram showing its associated mechanism network and possible changes in downstream factors.

4. Discussion

The pathogenesis and pathological processes of diabetes are complex and varied, and organ specificity is obvious, which has not been thoroughly examined thus far [19,20]. Research on disease-related signaling factors and functional networks by many international research teams has led to the targeted monitoring and treatment of diabetes in clinical practice. Although there have been numerous studies of transcriptional data from diabetic and healthy individuals, few studies have been performed on patients with diabetes after stem cell therapy. Our study investigated the therapeutic effect of ADSC treatment on diabetes-related liver disease, and the results suggested that ADSC treatment may have additional therapeutic effects on diabetes-induced liver injury and identified possible key pathways and important targets in this process.

We performed whole-transcriptome RNA-seq analysis of STZ-induced hyperglycemic rats treated with ADSCs. Furthermore, research into the biology of diabetes has revealed multiple signaling and functional perturbations that occur in response to ADSC therapy during the development of diabetes, showing many important signaling networks in diabetes. Our results revealed the enrichment of genes and pathways according to liver damage, hepatitis, liver steatosis, LF and other hepatic diseases, and changes in the endocrine system and lipid metabolism were also identified. Therefore, we sought to identify relevant factors through which stem cell therapy plays a role in ameliorating liver damage.

Upstream regulator analysis identified *DUSP1* as a factor that was significantly downregulated in the transcriptome. At the top of the hierarchy, mechanistic network analyses revealed that *DUSP1* activated several signaling pathways: the IL-12 complex, IL-1B, and TNF. Furthermore, silencing DUSP1 *in vitro* enhanced TNF-α and IL expression *in vivo* and increased the expression of other proinflammatory factors [21,22]; in contrast, inhibiting MAPKs and inflammatory gene expression occurring after *DUSP1* activation is an important feature of the effects of glucocorticoid [23,24]. *DUSP1* deficiency increases systemic levels of proinflammatory cytokines and can promote inflammatory infiltration, and increased *DUSP1* mRNA levels may moderate insulin resistance; this process may be related to TNF [25,26]. Interestingly, in contrast to the inhibitory effect of *DUSP1* on many genes associated with inflammation, *DUSP1* silencing positively regulated IL-12p40, an

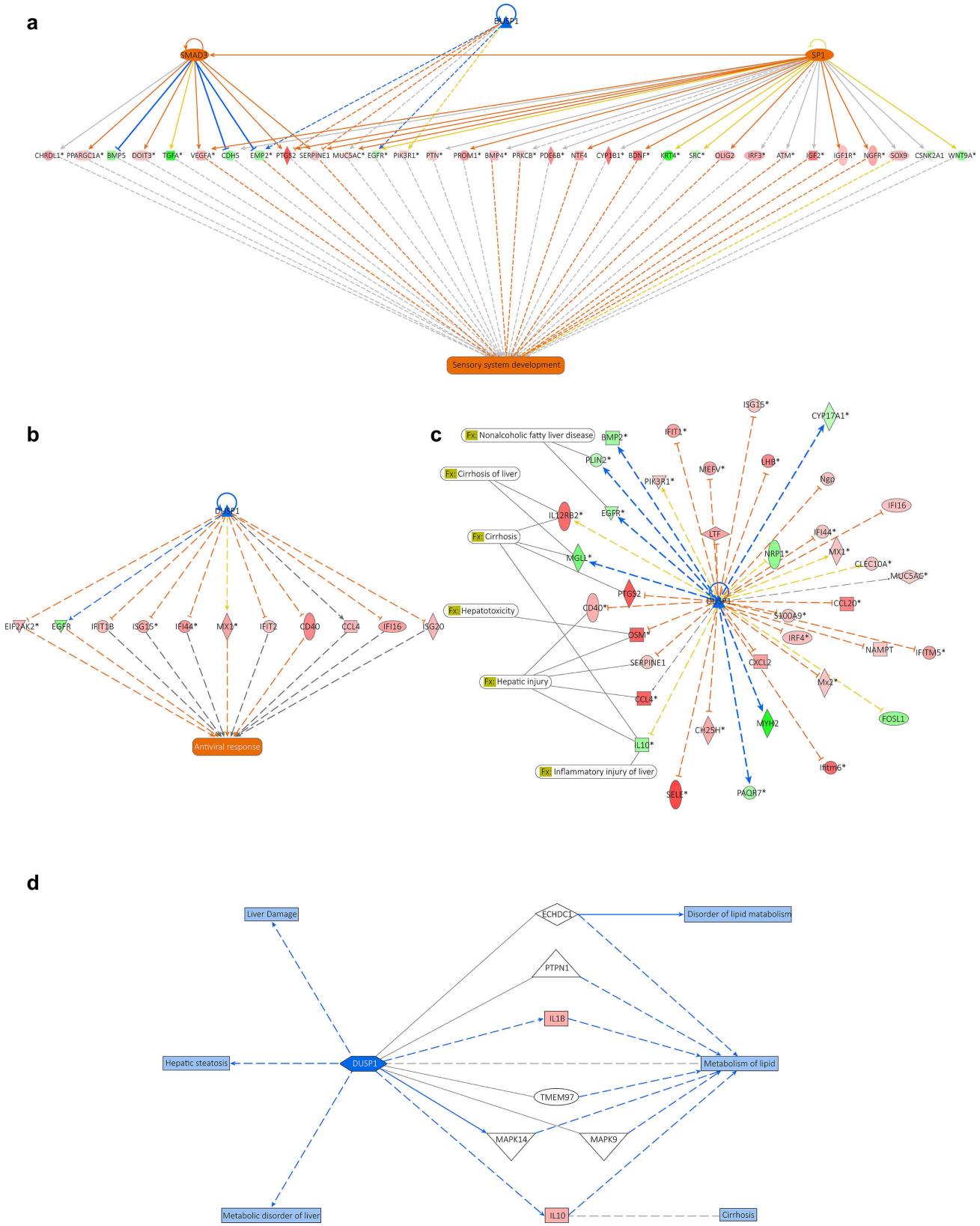

Fig. 6. Numerous disease-associated enrichment networks in diabetic rats. (a) Schematic of sensory system development and (b) antiviral response functional networks revealed by IPA. In this figure, red indicates activation, while blue indicates suppression. (c,d) DUSP1 is closely related to a variety of liver diseases and lipid metabolism disorders.

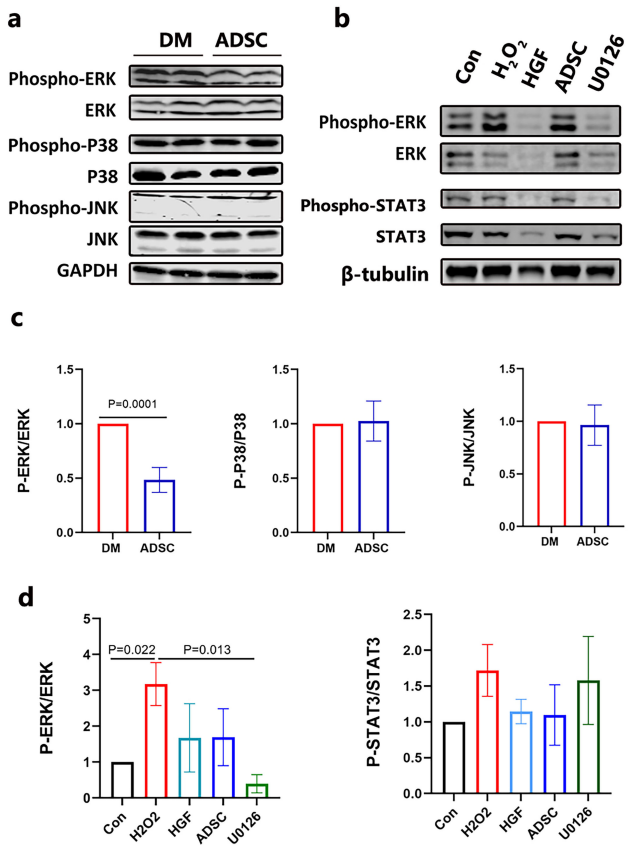

Fig. 7. Phosphorylation status of the ERK1/2, P38, JNK and STAT3 pathways. (a,c) The phosphorylation of ERK2, P38 and JNK in stem cell-treated diabetic rats and untreated diabetic rats. An unpaired t test was used to compare the two groups. (b,d) The phosphorylation of ERK1/2 and STAT3 in HGF- or stem cell-treated HepG2 cells induced by H_2O_2. An unpaired *t* test was used to compare the H_2O_2 group with the control (Con) group and the HGF, ADSC or U0126 groups with the H_2O_2 group. ERK, extracellular regulated protein kinase; JNK, c-jun N-terminal kinase; STAT3, signal transducer and activator of transcription 3; HGF, hepatocyte growth factor.

important factor in the activation of the Th1 response, suggesting that *DUSP1* modulates Th1 immune responses and plays a role in maintaining antimicrobial defense [27]. In summary, the involvement of *DUSP1* in insulin production and secretion and inflammation lays the foundation for its role in the diagnosis and treatment of diabetes.

Liver damage plays a key role in diabetes [28], which led us to further explore whether *DUSP1* was also involved in diabetic liver damage. Our data revealed a change in *DUSP1*, suggesting that *DUSP1* may be an important upstream factor affecting diabetic liver damage. A review of previous studies showed that *DUSP1* plays different roles in liver damage caused by different etiologies. Alcohol-induced downregulation of *DUSP1* in liver tissue was previously shown to further enhance TNF-α release and promote the progression of liver damage, which may be an important mechanism of alcoholic steatohepatitis (ASH) [29]. In contrast, dexmedetomidine treatment increased glycogen synthase kinase-3 (GSK-3)/*DUSP1*/nuclear factor erythroid 2-related factor 2 (NRF2) pathway activity, attenuated oxidative stress and apoptosis in the rat liver, and subsequently prevented liver damage [30]. This finding may indicate a complex mechanism of *DUSP1* in the involvement of diabetes-induced liver damage.

Mechanistic network analysis showed that the expression of several chemokines (including C-C motif chemokine ligand 4 (CCL4) and C-C motif chemokine ligand 20 (CCL20)) was changed in liver tissue after ADSC treatment compared with untreated diseased tissue. A study showed a potential connection between upregulated CCL4 expression, reduced cholesterol levels in liver tissue and the progression of liver damage, which is consistent with our results [31]. Moreover, massive secretion of CCL20 can activate the p38 MAPK pathway, thereby reducing inflammatory symptoms and improving liver repair in mice [32]. It was also found that inhibiting the chemokine CCL20 reduced immune cell infiltration and extracellular matrix (ECM) production, and ECM production actively promoted NASH progression [33]. In conclusion, altered chemokine expression in liver tissue has multiple consequences, including early liver damage, hepatitis, LF, and even liver cirrhosis.

On the other hand, our results suggest that the activation of another class of proinflammatory mediators, including IL-6, IL-1B, and TNF, has potential inhibitory activity against liver damage. Interestingly, the expression of IL-10, an anti-inflammatory cytokine, was bidirectionally altered in our study, which may indicate a complex mechanism that is active during the treatment of diabetic liver damage. Targeting IL-10 can not only prevent liver damage but also play a role in liver lipid metabolism dysregulation and liver cirrhosis. IL-10, which is preferentially expressed in natural killer cells and can alleviate liver damage to some extent, has been reported to have immunoregulatory effects [34]. Moreover, the receptors for some cytokines were also upregulated, such as Il12rb2. IL-12/IL-23-mediated Th1/Th17 signaling is implicated in the pathogenesis of primary biliary cirrhosis (PBC), and targeting Il12rb2 may alleviate but not reverse the progression of liver damage [35].

In addition to the aforementioned alterations in cytokines and chemokines, we also screened for specific genetic changes, which were to some extent corroborated by previous studies. Several reports have suggested that loss of the protein tyrosine phosphatase 1B (PTP1B) gene inhibits fas expression, which may contribute to resistance to liver damage and lethality [36], as well as to the treatment of lipotoxic liver damage [28]. Significant alterations were also found in MAPK14, an important member of the MAPK family. Despite the dual functions of MAPK14, in most cases, it has been shown that therapeutic targeting of MAPK14 can exert anti-inflammatory and antioxi-

dant effects on the liver by increasing the polarization of M2 macrophages, ultimately facilitating liver regeneration [37,38]. These factors showed a close correlation with *DUSP1* in the functional network identified by IPA. Then, we explored the possible signaling pathways regulated by *DUSP1*. *DUSP1* is related to the NLRP3 inflammasome in cerebral injury [39]. It was reported that mesenchymal stem cell-derived exosomes could block the malignant behaviors of hepatocellular carcinoma stem cells through the lncRNA C5orf66-AS1/microRNA-127-3p/DUSP1/ERK axis [40]. In the present study, we found that ADSCs decreased the phosphorylation levels of ERK1/2 and STAT3 in the livers of DM rats and in HepG2 cells induced by H_2O_2 (Fig. 7). These results suggest that the ERK pathway can mediate STAT3 and inflammatory factors involved in ADSC treatment of diabetic liver damage, which might be regulated by *DUSP1*.

5. Conclusions

In summary, the data in this study suggest that *DUSP1* plays an important role in the therapeutic effect of ADSCs on diabetes and that the effects of proinflammatory mediators such as IL-6, IL-1B, TNF and the NLRP3 inflammasome and anti-inflammatory factors such as IL-10 cannot be ignored. Therefore, our data highlight possible targets for ADSCs in diabetes treatment, and determining whether these targets and the related pathways can add to the current arsenal of treatments for diabetes requires further studies with larger sample sizes and clinical experiments.

Availability of Data and Materials

The datasets used and/or analyzed during the current study are available from the corresponding author on reasonable request.

Author Contributions

XW and DLiu designed the study, acquired funding, reviewed and edited the manuscript. YH and GG performed the research and wrote the manuscript. WD and PW analyzed the data. CL and DLin provided administrative support on the research. CL conducted animal experiments and DLin conducted cell culture and treatments. All authors contributed to editorial changes in the manuscript. All authors read and approved the final manuscript. All authors have participated sufficiently in the work to take public responsibility for appropriate portions of the content and agreed to be accountable for all aspects of the work in ensuring that questions related to its accuracy or integrity.

Ethics Approval and Consent to Participate

The animal study protocol was approved by the Ethics Committee of the Shandong Institute of Endocrine and Metabolic Diseases (2018-008, Oct 2018).

Acknowledgment

Not applicable.

Funding

This work was supported by the China National Natural Science Foundation, grant number 81900736; China Postdoctoral Science Foundation, grant number 2023M732137; Guidelines for Prevention and Intervention of Disability among the Elderly in Shandong Province; Qilu Geriatric Diseases Chinese and Western Academic School Inheritance Workshop Project (No.2022-93-1-10); and Postdoctoral Project of Shandong University of Traditional Chinese Medicine.

Conflict of Interest

The authors declare no conflict of interest.

Supplementary Material

Supplementary material associated with this article can be found, in the online version, at https://doi.org/10.31083/j.fbl2812365.

References

[1] Katsarou A, Gudbjörnsdottir S, Rawshani A, Dabelea D, Bonifacio E, Anderson BJ, *et al*. Type 1 diabetes mellitus. Nature Reviews. Disease Primers. 2017; 3: 17016.

[2] Sun H, Saeedi P, Karuranga S, Pinkepank M, Ogurtsova K, Duncan BB, *et al.* IDF Diabetes Atlas: Global, regional and country-level diabetes prevalence estimates for 2021 and projections for 2045. Diabetes Research and Clinical Practice. 2022; 183: 109119.

[3] Tomic D, Shaw JE, Magliano DJ. The burden and risks of emerging complications of diabetes mellitus. Nature Reviews Endocrinology. 2022; 18: 525–539.

[4] Stefan N, Cusi K. A global view of the interplay between non-alcoholic fatty liver disease and diabetes. Lancet Diabetes & Endocrinology. 2022; 10: 284–296.

[5] Thompson AJ, Patel K. Antifibrotic Therapies: will we ever Get there? Current Gastroenterology Reports. 2010; 12: 23–29.

[6] Leng Z, Zhu R, Hou W, Feng Y, Yang Y, Han Q, *et al*. Transplantation of ACE2- Mesenchymal Stem Cells Improves the Outcome of Patients with COVID-19 Pneumonia. Aging and Disease. 2020; 11: 216.

[7] Sengupta V, Sengupta S, Lazo A, Woods P, Nolan A, Bremer N. Exosomes Derived from Bone Marrow Mesenchymal Stem Cells as Treatment for Severe COVID-19. Stem Cells and Development. 2020; 29: 747–754.

[8] Shu L, Niu C, Li R, Huang T, Wang Y, Huang M, *et al*. Treatment of severe COVID-19 with human umbilical cord mesenchymal stem cells. Stem Cell Research & Therapy. 2020; 11: 361.

[9] Takahashi H, Sakata N, Yoshimatsu G, Hasegawa S, Kodama S. Regenerative and Transplantation Medicine: Cellular Therapy Using Adipose Tissue-Derived Mesenchymal Stromal Cells for Type 1 Diabetes Mellitus. Journal of Clinical Medicine. 2019; 8: 249.

[10] Jin J, Shi Y, Gong J, Zhao L, Li Y, He Q, *et al*. Exosome secreted from adipose-derived stem cells attenuates diabetic nephropathy by promoting autophagy flux and inhibiting apoptosis in podocyte. Stem Cell Research & Therapy. 2019; 10: 95.

[11] Hou Y, Ding W, Wu P, Liu C, Ding L, Liu J, *et al*. Adipose-

derived stem cells alleviate liver injury induced by type 1 diabetes mellitus by inhibiting mitochondrial stress and attenuating inflammation. Stem Cell Research & Therapy. 2022; 13: 132.
[12] Warshauer JT, Belk JA, Chan AY, Wang J, Gupta AR, Shi Q, *et al*. A human mutation in STAT3 promotes type 1 diabetes through a defect in CD8+ T cell tolerance. The Journal of Experimental Medicine. 2021; 218: e20210759.
[13] Gribben C, Lambert C, Messal HA, Hubber EL, Rackham C, Evans I, *et al*. Ductal Ngn3-expressing progenitors contribute to adult β cell neogenesis in the pancreas. Cell Stem Cell. 2021; 28: 2000–2008.e4.
[14] He F, Huang Y, Song Z, Zhou HJ, Zhang H, Perry RJ, *et al*. Mitophagy-mediated adipose inflammation contributes to type 2 diabetes with hepatic insulin resistance. Journal of Experimental Medicine. 2021; 218: e20201416.
[15] Wang D, Yin Y, Wang S, Zhao T, Gong F, Zhao Y, *et al*. FGF1-HBS prevents diabetic cardiomyopathy by maintaining mitochondrial homeostasis and reducing oxidative stress via AMPK/Nur77 suppression. Signal Transduction and Targeted Therapy. 2021; 6: 133.
[16] Kelley N, Jeltema D, Duan Y, He Y. The NLRP3 Inflammasome: An Overview of Mechanisms of Activation and Regulation. International Journal of Molecular Sciences. 2019; 20: 3328.
[17] Fusco R, Siracusa R, Genovese T, Cuzzocrea S, Di Paola R. Focus on the Role of NLRP3 Inflammasome in Diseases. International Journal of Molecular Sciences. 2020; 21: 4223.
[18] Kang YJ, Bang BR, Otsuka M, Otsu K. Tissue-Specific Regulation of p38α-Mediated Inflammation in Con a–Induced Acute Liver Damage. Journal of Immunology. 2015; 194: 4759–4766.
[19] Forbes JM, Cooper ME. Mechanisms of Diabetic Complications. Physiological Reviews. 2013; 93: 137–188.
[20] Harcourt BE, Penfold SA, Forbes JM. Coming full circle in diabetes mellitus: from complications to initiation. Nature Reviews Endocrinology. 2013; 9: 113–123.
[21] Salojin KV, Owusu IB, Millerchip KA, Potter M, Platt KA, Oravecz T. Essential Role of MAPK Phosphatase-1 in the Negative Control of Innate Immune Responses. The Journal of Immunology. 2006; 176: 1899–1907.
[22] Zhang B, Li SL, Xie HL, Fan JW, Gu CW, Kang C, *et al*. Effects of silencing the DUSP1 gene using lentiviral vector-mediated siRNA on the release of proinflammatory cytokines through regulation of the MAPK signaling pathway in mice with acute pancreatitis. InternationalJournal of Molecular Medicine. 2018; 41: 2213–2224.
[23] Clark AR, Martins JRS, Tchen CR. Role of Dual Specificity Phosphatases in Biological Responses to Glucocorticoids. Journal of Biological Chemistry. 2008; 283: 25765–25769.
[24] Shah S, King EM, Chandrasekhar A, Newton R. Roles for the Mitogen-activated Protein Kinase (MAPK) Phosphatase, DUSP1, in Feedback Control of Inflammatory Gene Expression and Repression by Dexamethasone. Journal of Biological Chemistry. 2014; 289: 13667–13679.
[25] Vandevyver S, Dejager L, Van Bogaert T, Kleyman A, Liu Y, Tuckermann J, *et al*. Glucocorticoid receptor dimerization induces MKP1 to protect against TNF-induced inflammation. Journal of Clinical Investigation. 2012; 122: 2130–2140.
[26] Fujimoto S, Mochizuki K, Shimada M, Hori T, Murayama Y, Ohashi N, *et al*. Insulin resistance induced by a high-fat diet is associated with the induction of genes related to leukocyte activation in rat peripheral leukocytes. Life Sciences. 2010; 87: 679–685.
[27] Korhonen R, Huotari N, Hömmö T, Leppänen T, Moilanen E. The expression of interleukin-12 is increased by MAP kinase phosphatase-1 through a mechanism related to interferon regulatory factor 1. Molecular Immunology. 2012; 51: 219–226.
[28] Barahona I, Rada P, Calero-Pérez S, Grillo-Risco R, Pereira L, Soler-Vázquez MC, *et al*. Ptpn1 deletion protects oval cells against lipoapoptosis by favoring lipid droplet formation and dynamics. Cell Death & Differentiation. 2022; 29: 2362–2380.
[29] Ajakaiye MA, Jacob A, Wu R, Zhou M, Ji Y, Dong W, *et al*. Upregulation of Kupffer cell α2a-Adrenoceptors and downregulation of MKP-1 mediate hepatic injury in chronic alcohol exposure. Biochemical and Biophysical Research Communications. 2011; 409: 406–411.
[30] Sha J, Zhang H, Zhao Y, Feng X, Hu X, Wang C, *et al*. Dexmedetomidine attenuates lipopolysaccharide-induced liver oxidative stress and cell apoptosis in rats by increasing GSK-3β/MKP-1/Nrf2 pathway activity via the α2 adrenergic receptor. Toxicology and Applied Pharmacology. 2019; 364: 144–152.
[31] Otrubová O, Turecký L, Uličná O, Janega P, Luha J, Muchová J. Therapeutic effects of N-acetyl-L-cysteine on liver damage induced by long-term CCl4 administration. General Physiology and Biophysics. 2018; 37: 23–31.
[32] Wang Y, Xie X, Liu H, Liu H, Jiang H. LR12 Promotes Liver Repair by Improving the Resolution of Inflammation and Liver Regeneration in Mice with Thioacetamide- (TAA-) Induced Acute Liver Failure. Mediators of Inflammation. 2021; 2021: 2327721.
[33] Ryu J, Kim E, Kang MK, Song DG, Shin EA, Lee H, *et al*. Differential TM4SF5-mediated SIRT1 modulation and metabolic signaling in nonalcoholic steatohepatitis progression. The Journal of Pathology. 2021; 253: 55–67.
[34] Ali AK, Komal AK, Almutairi SM, Lee SH. Natural killer cell-derived IL-10 prevents liver damage during sustained murine cytomegalovirus infection. Frontiers in immunology. 2019; 10: 2688.
[35] Yang C, Ma X, Tsuneyama K, Huang S, Takahashi T, Chalasani NP, *et al*. IL-12/Th1 and IL-23/Th17 biliary microenvironment in primary biliary cirrhosis: Implications for therapy. Hepatology. 2014; 59: 1944–1953.
[36] Sangwan V, Paliouras GN, Cheng A, Dubé N, Tremblay ML, Park M. Protein-tyrosine Phosphatase 1B Deficiency Protects against Fas-induced Hepatic Failure. Journal of Biological Chemistry. 2006; 281: 221–228.
[37] Campbell JS, Argast GM, Yuen SY, Hayes B, Fausto N. Inactivation of p38 MAPK during liver regeneration. The International Journal of Biochemistry & Cell Biology. 2011; 43: 180–188.
[38] Schulze-Osthoff K, Bantel H. Macrophage p38 kinase inhibition for liver regeneration. The FEBS Journal. 2017; 284: 4196–4199.
[39] Fan W, Qin Y, Tan J, Li B, Liu Y, Rong J, *et al*. RGD1564534 represses NLRP3 inflammasome activity in cerebral injury following ischemia-reperfusion by impairing miR-101a-3p-mediated Dusp1 inhibition. Experimental Neurology. 2023; 359: 114266.
[40] Gu H, Yan C, Wan H, Wu L, Liu J, Zhu Z, e*t al.* Mesenchymal stem cell-derived exosomes block malignant behaviors of hepatocellular carcinoma stem cells through a lncRNA C5orf66-as1/microRNA-127-3p/DUSP1/ERK axis. Human Cell. 2021; 34: 1812–1829.